https://doi.org/10.5194/egusphere-2026-2434
Preprint. Discussion started: 19 June 2026

Dust Record from Allan Hills Blue Ice: Towards Extending the Archive to 4000 ka

Alissa Choi[1†], Austin J. Carter[2,3†], Julia Marks-Peterson[4], Sarah Shackleton[3,5], John A. Higgins[3], Edward J. Brook[4], Liam Kirkpatrick[6], Jacob I. Chalif[7], Sarah M. Aarons[2,8,9]

[1]Department of Geoscience, University of Wisconsin Madison, Madison, WI 53706, United States
[2]Scripps Institution of Oceanography, University of California San Diego, La Jolla, CA 92093, United States
[3]Department of Geosciences, Princeton University, Princeton, NJ 08544, United States
[4]College of Earth, Ocean, and Atmospheric Sciences, Oregon State University, Corvallis, OR 97331, United States
[5]Department of Geology and Geophysics, Woods Hole Oceanographic Institution, Woods Hole, MA 02543, United States
[6]Department of Earth and Space Sciences, University of Washington, Seattle, 98195, United States
[7]Department of Earth and Planetary Sciences, Dartmouth College, Hanover, 03755, United States
[8]Lamont-Doherty Earth Observatory, Columbia University, Palisades, NY, 10964, United States
[9]Department of Earth and Environmental Sciences, Columbia University, New York, NY, 10027, United States
†These authors contributed equally to this work.

Correspondence to: ac6202@columbia.edu; ac2889@princeton.edu

Abstract

Previous analyses of dust concentration and size distribution in ice cores are limited to the past 800,000 years; however, the ALHIC1901 ice core drilled at the Allan Hills Blue Ice Area (BIA) in East Antarctica provides a unique opportunity to examine older discontinuous records of ice ranging in age from 4000–500 ka. Here we present a discrete record of insoluble particles within ALHIC1901 from the bottom 25 m of the core. We investigated the particle mass concentration, size distribution, and mineralogy within the core to assess the preservation of dust records in BIAs with complex flow histories. We find that the insoluble particle concentrations are likely altered by entrainment of basal sediment for depths 5 m above bedrock. For shallower depths less affected by subglacial input, the record lacks expected peaks in dust concentration during glacial periods, which have been termed "long snapshots," implying that low net accumulation rates during glacial periods at the Allan Hills BIA results in the preferential loss or attenuation of glacial ice and a corresponding bias toward the preservation of interglacial ice. The dust concentrations may also be further smoothed due to ice thinning. A subset of particles from both the upper and lower ranges of depths analyzed shows evidence of mineral weathering and/or *in situ* production of secondary minerals, and insoluble particle concentration correlates well with

https://doi.org/10.5194/egusphere-2026-2434
Preprint. Discussion started: 19 June 2026

non-atmospherically derived carbon dioxide concentrations. These results highlight the importance of identifying signs of basal ice-rock interactions and/or complicated accumulation and ablation histories as these affect our interpretation of paleoclimate records preserved in ice cores from BIAs.

1 Introduction

One motivation to study Earth's past climate variability is rooted in the need to better understand how Earth systems may respond to contemporary and future climate change. A key moment in Earth's climate history is the Mid-Pleistocene Transition (MPT; ~1.25–0.7 Ma) when glacial-interglacial cycles lengthened from 40 kyr to 100 kyr and glacial periods intensified (Shackleton & Opdyke, 1977; Medina-Elizalde & Lea, 2005; Clark et al., 2006; Elderfield et al., 2012; Past Interglacials Working Group of PAGES, 2016). Though this change in response to orbital forcing is clearly captured in the stable oxygen isotope record of marine sediment cores, uncertainties in drivers of this change as well as its effect on Earth system couplings remain elusive (Clark and Pollard 1998; Elderfield et al., 2012; Past Interglacials Working Group of PAGES, 2016).

The effort to reconstruct past dust flux to marine and terrestrial ecosystems during critical paleoclimate transitions is also rooted in the fact that dust-borne iron (Fe) is a major micronutrient in high-nutrient low-chlorophyll areas of the ocean such as the Southern Ocean. Iron fertilization of phytoplankton increases atmospheric CO_2 uptake through photosynthesis (Martin et al., 1990; Martínez-Garcia et al., 2014; 2011; 2009; Jaccard et al., 2013; Sigman et al., 2010) and an increase in the dust flux delivered to the Southern Ocean has been invoked as a potential driver of the MPT (Martínez-Garcia et al.,, 2011), with mass accumulation rates of dust and Fe in marine sediments used to probe how dust delivery may influence the global carbon cycle on long timescales (Martínez-Garcia et al., 2014; 2011; 2009; Jaccard et al., 2013; Sigman et al., 2010). Following dust deposition in the surface ocean, potential post-depositional changes in dust chemistry and speciation during transport through the water column (Bressac & Guieu, 2013) underpin the need to reconstruct dust records using relatively pristine Antarctic ice cores. Existing marine sediment records of Southern Hemisphere dust span millions of years (Martínez-Garcia et al., 2014; 2011), however ice cores provide a higher temporally resolved and relatively pristine archive of dust deposition on shorter thousand-year timescales (e.g., Lambert et al., 2008). Increasing the spatial

https://doi.org/10.5194/egusphere-2026-2434
Preprint. Discussion started: 19 June 2026

coverage of dust records beyond the Southern Ocean and comparing the records of coastal versus interior East Antarctica are therefore needed to gauge how dust delivery varied regionally during major climate transitions. Finally, dust concentration measurements can be coupled directly with atmospheric CO_2 measurements in ice cores allowing us to directly probe the relationship between shifts in dust flux/composition and atmospheric CO_2.

Ice cores provide an opportunity to reconstruct robust records of past climate during the Pleistocene and earlier through multi-proxy approaches which include measurements of atmospheric gas composition, stable isotopic composition of water, and mineral dust, which can inform us on regional and global atmospheric circulation (Mahowald et al., 1999). The composition and flux of aeolian mineral dust deposited upon ice sheet surfaces varies depending on climate regime, with extreme fluctuations occurring across glacial–interglacial cycles (Lambert et al., 2008). Throughout Antarctica, ice formed during glacial periods is characterized by a higher concentration of fine (1–5 µm diameter) dust from mid-latitude sources (Delmonte et al., 2007), due to a combination of more vigorous atmospheric circulation and a weakened hydrological cycle resulting in a drier climate (McGee et al., 2010; Steffensen 1997; Kea 1994). Antarctic ice from interglacial periods contains significantly lower dust mass concentrations than glacial ice (e.g., Lambert et al., 2008), making geochemical and isotopic measurements on this dust more challenging. Compared to glacial ice, dust particles from interglacial ice at interior Antarctic sites remain smaller than 5 µm in diameter but contain a greater proportion (7–10%) of 3–5 µm particles (Delmonte et al., 2007). In contrast, interglacial ice at peripheral East Antarctic sites is dominated by the presence of much coarser particles (5–20 µm), indicative of strengthened transport of local Antarctic material and diminished mid-latitude dust transport (Aarons et al., 2017; Albani et al., 2012; Delmonte et al., 2010; Carter et al., accepted).

Shifts in dust concentration and size distribution as a function of climate regimes are consistently observed in ice cores retrieved from interior portions of the East Antarctic Ice Sheet (EAIS) such as the EPICA Dome C (EDC) and Vostok cores. These shifts are a first-order signifier of climate regimes and could theoretically be used as a tool for dating ice when coupled with a reference record such as a marine sediment core (Ng et al., 2024). Ice core dust concentration can be used to infer whether ice was formed during a glacial or interglacial period due to the tight coupling of Antarctic and lower-latitude climate (Lambert et al., 2008, Delmonte et al., 2004),

https://doi.org/10.5194/egusphere-2026-2434
Preprint. Discussion started: 19 June 2026

highlighting the utility of dust concentrations as a gauge on climate and temperature. Dust grain size distributions are often used to indicate wind speeds and degree of storminess (Steffensen, 1997), both of which may influence the amount of local or regional dust transported to an ice core site.

Ice core dust proxy reconstructions are generally considered to be pristine, uncomplicated by post-depositional processes or ice flow. With increasing age comes the possibility of complicated ice flow histories, and old ice at BIAs are particularly well known for disturbances in their stratigraphic layering (Fig. 1; Shackleton et al., 2025; Higgins et al., 2015; Yan et al., 2019). Because the oldest continuous ice core record in the Southern Hemisphere (EDC) extends only to ~800 ka, our understanding of dust transport and dynamics on geologic timescales is limited beyond this time frame. Here, we present a new record of dust deposition to the Allan Hills Blue Ice Area (BIA) using the ALHIC1901 ice core, which spans approximately 4000–500 ka (Shackleton et al., 2025), providing snapshots of the dust concentration record older than the 800-ka record (Lambert et al., 2008). We critically evaluate the dust record throughout the deepest 25 meters of ALHIC1901 above bedrock, which contains the oldest sections of ice. We then compare our dust concentration and size distribution measurements to continuous, well-dated dust records (ALHIC1903) from the Allan Hills BIA (Carter et al., accepted) and EDC (Lambert et al., 2008) and with existing CO_2 data on samples from the same ice core at equal depths (Marks-Peterson et al., 2026). In doing so, we find that the climate signals preserved in this ice core are complicated by two distinct processes: (1) in the deepest ice (<5 m above bed), there is non-aeolian particle entrainment from subglacial sources, many of which have undergone secondary mineralization and/or *in situ* chemical weathering processes and (2) at shallower depths, there is an interglacial bias driven by low accumulation and high ablation rates at the Allan Hills site (Fig. 1).

https://doi.org/10.5194/egusphere-2026-2434
Preprint. Discussion started: 19 June 2026

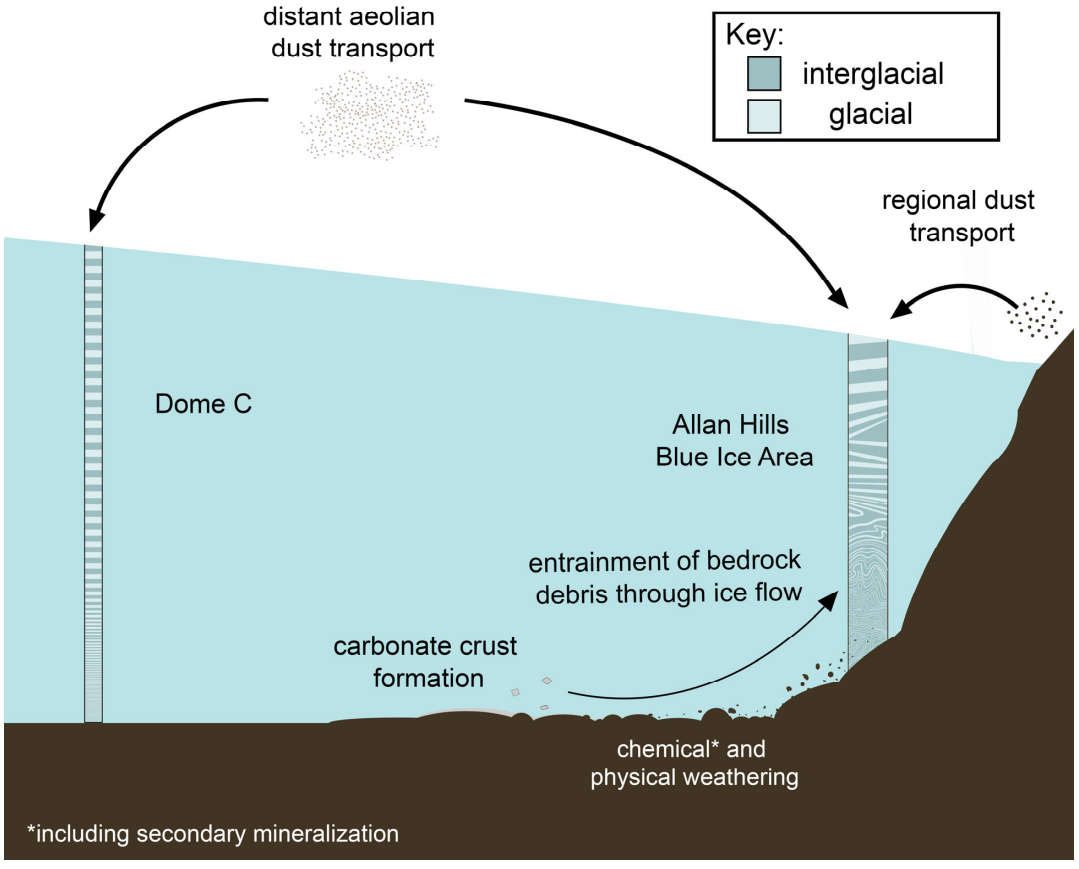

Figure 1. Schematic outlining hypotheses presented in this study associated with interpretations of dust records from deformed Blue Ice Areas specifically the Allan Hills compared to continuous records such as EPICA Dome C. Discontinuous stratigraphy of the Allan Hills is shown with increasing age density throughout the depth transition. Note: depictions of exact flow regimes and stratigraphy are for illustrative purposes only and not drawn to scale.

2 Methods

2.1 Site description and sampling

The Allan Hills BIA is a peripheral Antarctic site adjacent to the Convoy Range of the Transantarctic Mountains draining the EAIS. Here a combination of unique glaciological and climatic conditions, including the complex underlying bedrock topography and high surface

https://doi.org/10.5194/egusphere-2026-2434
Preprint. Discussion started: 19 June 2026

ablation rates, allows for the preservation of discontinuous sections of ice dating back to 6000 ka in shallow (<200 m) cores (Shackleton et al., 2025, Yan et al., 2019, Higgins et al., 2015). The present-day average accumulation rate at the Allan Hills is ~0.0075 m yr^{-1} and the average ablation rate is 0.02 m yr^{-1}, resulting in a net negative mass balance (Dadic et al., 2015, Spaulding et al., 2012, Spaulding et al., 2013). During the 2019–2020 field season, the ALHIC1901 ice core (76.732376° S, 159.356125° E, 1991.1 m.a.s.l.) was drilled ~160 m to bedrock at the Allan Hills BIA (Fig. 2). The core was drilled using the National Science Foundation (NSF) Ice Drilling Program (IDP) Blue Ice Drill, which has a core diameter of 24.1 cm (Kuhl et al., 2014). The core was transported to the NSF Ice Core Facility (NSF-ICF) in Lakewood, CO for processing and long-term storage. The ice core samples analyzed in this study (n=95) were subsampled using bandsaws at the NSF-ICF and at Princeton University, and the resulting subsamples ranged in mass from 50–150 g. At Scripps Institution of Oceanography (SIO) samples were stored at -25°C prior to analysis.

https://doi.org/10.5194/egusphere-2026-2434
Preprint. Discussion started: 19 June 2026

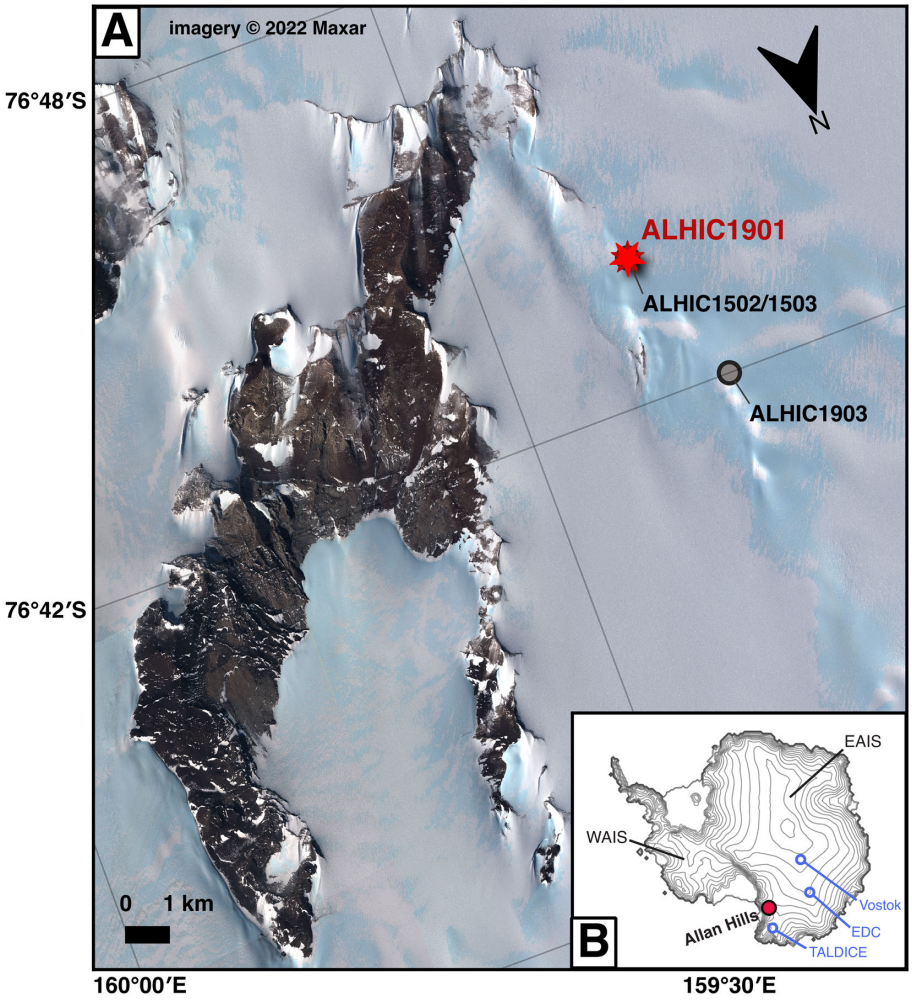

Figure 2. (**A**) Site map of the Allan Hills Blue Ice Area including the ALHIC1901 ice core (red star; this study) and additional ice coring sites referenced in this text (gray circles). Imagery © 2022 Maxar. Note that ALHIC1901 is a companion core drilled in the vicinity of the ALHIC1502 and ALHIC1503 ice cores (Higgins et al., 2015; Yan et al., 2019), hence the overlapping markers. (**B**) Inset map of Antarctica adapted from Steig et al. (2015) showing the location of the Allan Hills for added context. The West Antarctic Ice Sheet (WAIS) and East Antarctic Ice Sheet (EAIS) are noted with the latter including deeper ice coring sites referenced in the text as blue open circles.

https://doi.org/10.5194/egusphere-2026-2434
Preprint. Discussion started: 19 June 2026

2.2 Coulter Counter analysis

Each sample was analyzed for mass concentration and grain size distribution at SIO following established ice core procedures (Carter et al., accepted; Delmonte et al., 2004; Steffensen et al., 1997). The ice subsamples were transported from storage to an ISO Class 7 cleanroom at the Climate and Earth Surface Geochemistry Lab at SIO. Prior to melting, samples were cleaned by rinsing with ultrapure water (18.2 MΩ·cm) over the surface area two to three times. After rinsing, the subsamples were placed in acid precleaned PFA jars. Each subsample was then allowed to melt and acclimate to room temperature. For masses larger than 100 g, an infrared heat lamp was used to accelerate the melting process. Following melting, the liquid subsample was gently agitated to ensure a homogenous mixture of particles prior to analysis. A sample volume of 10 mL was transferred into an accuvette cleaned by twice rinsing with ultrapure water and once with ISOTON™ II (~1% NaCl solution). To make each subsample conductive, 0.5 mL of a 20% NaCl solution (prefiltered through a 0.02 µm membrane) was added to the accuvette, resulting in a ~1% NaCl solution.

Samples were then analyzed for mass concentration and grain size distribution of insoluble particulate matter using a Beckman Multisizer 4e Coulter Counter at SIO. The instrument works by passing a metered volume of conductive solution through an aperture, which is under constant voltage. Voltage pulses are detected when a particle passes through the aperture due to a change in electrical resistance. The quantity of pulses reflect particle quantity and pulse height is proportional to particle volume. Each individual sample was analyzed a minimum of 5 times using an analytical volume of 0.5 mL and a 50 µm aperture tube. We report the average concentration and grain size distribution across 400 bins of particle diameter size logarithmically spaced from 1 to 30 µm. Samples that initially read an abnormal final particle count number as well as those that resulted in instrumental error due to blockage of the aperture hole were run a greater number of times to ensure accuracy of data. Data from individual sample runs that encountered blockages were discarded due to potential errors in the collected data.

To determine the number of particles per mL for each size bin i (N_i), the measured number of particles in each bin (n_i) was normalized by the analytical volume (V_a, mL) and corrected for dilution using a dilution factor (DF) based on the sample and electrolyte volumes (V_s and V_e).

https://doi.org/10.5194/egusphere-2026-2434
Preprint. Discussion started: 19 June 2026

$$N_i = \frac{n_i}{V_a} \times DF \quad (1)$$

where N_i is the number of particles per mL in bin i. The dilution factor was calculated as:

$$DF = \frac{V_s + V_e}{V_s} \quad (2)$$

Total particle volume per mL for each size bin (V_i, µm^3 mL^{-1}) was then calculated with the assumption that particles are spherical and using the midpoint diameter of each bin (d_i):

$$V_i = N_i \times \frac{4}{3}\pi\left(\frac{d_i}{2}\right)^3 \quad (3)$$

Finally, total particle mass per mL for each bin (M_i, ng mL^{-1}, equivalent to parts per billion, ppb) was calculated from particle volume assuming an average density of continental crust (ρ_c = 2.5 x 10^{-3} ng µm^{-3}; Christensen and Mooney 1995):

$$M_i = \rho_c \times V_i \quad (4)$$

Between the five sample analyses, the aperture tube was flushed and unblocked to ensure the aperture opening was devoid of any remaining particles. Flushing the aperture reduces the risk of blockages during sample analysis which may inhibit the ability of particles to pass through the aperture and result in an inaccurate particle count. Samples were also occasionally lightly agitated prior to analysis to prevent gravitational settling of dust particles which would result in artificially lower measured dust concentrations. Between sample runs, the aperture tube was flushed twice and unblocked. In cases where samples were characterized by anomalously high final particle count numbers and frequent blockages, the aperture tube was re-cleaned by flushing and unblocking in 0.1 um and 0.2 µm filtered ISOTON™ II solution. Finally, the aperture tube was removed and cleaned daily prior to use by scrubbing with Coulter Clenz® cleaning agent. Blanks to evaluate the instrument stability over the measurement period were prepared daily before running any samples with 10 mL of 0.2 µm filtered ISOTON™ II and 0.5 mL 0.02 µm filtered 20% NaCl to evaluate the extent of external input of particles. The ISOTON™ II blanks were

https://doi.org/10.5194/egusphere-2026-2434
Preprint. Discussion started: 19 June 2026

consistently low throughout the entirety of the measurement period. A procedural blank was evaluated using 0.5 mL of 20% NaCl and 10 mL of 0.02 µm filtered ultrapure water. A background correction was applied for each particle diameter bin by subtracting the total blank count distribution from the count distribution of each sample. The influence of the blank correction was minor, representing on average only 2% of the total particles per mL of a sample. When not in use, the aperture tube was stored in 10 mL of 0.2 µm filtered ISOTON™ II solution.

2.3 Scanning electron microscopy (SEM) analysis

Residual sample meltwater was utilized for SEM analysis. The SEM samples were prepared following previously established methods (Gabriel et al., 2024). Approximately 1–5 mL of melt water from four selected samples was transferred into the center of a plastic ring form with a piece of Kapton tape on the underside. The sample was then dried on a hot plate set at 60°C. The sample was removed and cooled to room temperature prior to pouring epoxy resin mixture. Once the resin completed curing (up to 72 hours), the Kapton tape was carefully removed. Backscattered electron images were acquired at 2048-pixel resolution using a Phenom Pro XL SEM at 15 kV using a 60 µm diameter final aperture and 60 Pa vacuum. Semi-quantitative elemental composition was acquired for select particle features using point analysis and the equipped energy-dispersive X-ray spectroscopy (EDS) system.

3 Results and Discussion

3.1 Particle mass concentration with depth at the Allan Hills

Particle mass concentrations in ALHIC1901 span several orders of magnitude, ranging from ~60 to 12,000 ppb (Fig. 3). In the upper portion of the core (~135–140 m), concentrations range from ~90 to ~575 ppb, with frequent excursions above 300 ppb. Concentrations stabilize between ~140–150 m depth, where values are consistently low (100–220 ppb) with only rare, isolated excursions to higher concentrations at a few discrete depths (142.2 and 147.0 m). Below ~150 m, concentrations become progressively higher and more variable, culminating in a major shift at 154.9 m depth, where particle mass concentrations increase abruptly by more than an order

https://doi.org/10.5194/egusphere-2026-2434
Preprint. Discussion started: 19 June 2026

of magnitude. Below this boundary, concentrations remain persistently elevated, commonly exceeding 1000 ppb and reaching several thousand ppb toward the bottom of the core.

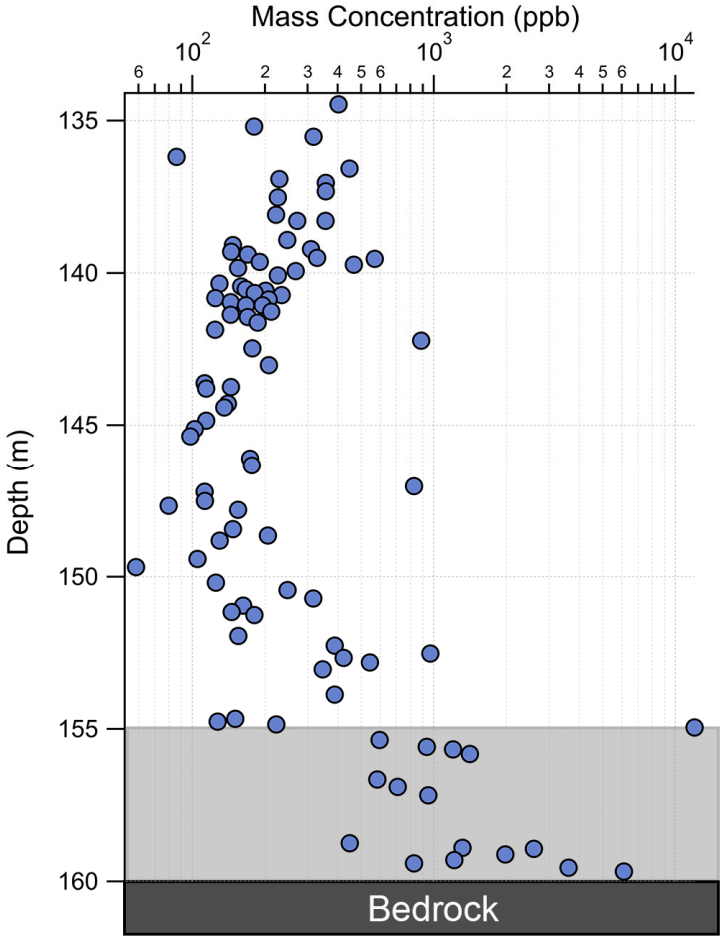

Figure 3. Total particle mass concentration of diameter range of 1-30 µm (blue circles; ng particles per g ice; ppb) in ALHIC1901 ice core samples on a logarithmic scale. Light gray shading highlights depths which may be influenced by basal contamination, and the dark gray rectangle represents the depth of bedrock.

The higher sustained dust concentrations (>1000 ppb) observed below 155 m are uncharacteristic of typical aeolian dust deposition to the Allan Hills BIA, which generally alternates from ~100 ppb during interglacial periods to as high as ~1000 ppb during glacial periods (Carter et al., accepted). In samples located within approximately 5 m from bedrock, the high particulate mass concentration was observable to the naked eye during the agitation process prior

https://doi.org/10.5194/egusphere-2026-2434
Preprint. Discussion started: 19 June 2026

to measurement using the Coulter Counter. Visible evidence of silt, sand, and, occasionally, a few pebble-sized particles that ranged from 0.1 to 10 mm were also present within these samples. These coarser grains were not possible to quantify given the aperture upper limit of 30 µm.

3.2 Size distribution evidence for basal contamination

Aeolian dust is often formed in arid areas, or in the case of the Southern Hemisphere much of the atmospherically transported dust is associated with glaciofluvial processes in Southern South America (SSA; Delmonte et al., 2004) traveling thousands of kilometers prior to deposition on the Antarctic Ice Sheet. The long transport distance of the primary contributor of aeolian dust (SSA) to Antarctica results in particle size sorting as many of the larger particles gravitationally settle out of the atmosphere closer to the dust source area (Delmonte et al., 2010). While mid-latitude sourced particles are predominately <5 µm, dust originating more locally from coastal ice-free areas throughout Antarctica can contain particles >5 µm in diameter (Delmonte et al., 2010). In ice core records, dust deposited during glacial periods is typically characterized by a distinctive lognormal distribution of mass concentrations close to 2 µm in diameter (Basile et al., 1997; Delmonte et al., 2004a). Dust records from interglacial intervals of coastal Antarctic ice cores are typically characterized by a reduced presence of fine particles (1–5 µm) and a greater overall presence of larger dust particle diameters (>5 µm) (Aarons et al., 2017; Carter et al., accepted; Albani et al., 2012).

The dust particle size can also be a first-order indicator of the presence of particles incorporated into the ice via entrainment of subglacial debris, as glacial abrasion can produce silt-sized particles (~2–63 µm) which can exceed the predominant diameter range of aeolian transported dust particles observed in previously studied Antarctic ice core records (e.g., 0.2–10 µm; Aarons et al., 2017). This subglacial sediment forms through intense physical weathering through glacial grinding, producing particles that typically contain a higher proportion of primary minerals, assuming there is little to no chemical weathering or water-rock interaction occurring in the subglacial environment (Knight, 1997). Sediment could then be incorporated into the ice itself in bands of debris along shear planes resulting in overall upward transport (Kassab et al., 2019, Kaplan et al., 2023). Although there is overlap in the particle diameters produced from during aeolian processes and glacial abrasion, the presence of particles greater than 10 µm in diameter

https://doi.org/10.5194/egusphere-2026-2434
Preprint. Discussion started: 19 June 2026

would imply either input from a proximal dust source area (e.g., locally exposed sediment within several kilometers of ice core drilling site) or basal debris entrainment (hereafter also referred to interchangeably as basal sediment). Analysis of size distribution alone is insufficient to disentangle the relative contributions of these potential sources.

Mass concentrations within 400 logarithmically spaced particle diameter ranges are normalized by bin spacing and then converted to a weighted percentage by dividing by the total particle mass concentration for each sample (Fig. 4) in order to determine which particle diameter ranges dominate the mass for each sample. Above the bottom 5 m basal section of ice (i.e., between ~135-155 m), samples at varying depths are a mix of either dominantly fine particle (1–5 µm) mass contributions or intermittently spaced coarse particle (>5 µm) mass contributions. In isolation, the patterns observed at these depths suggest the preservation of a climate signal (i.e., glacial and/or interglacial variability).

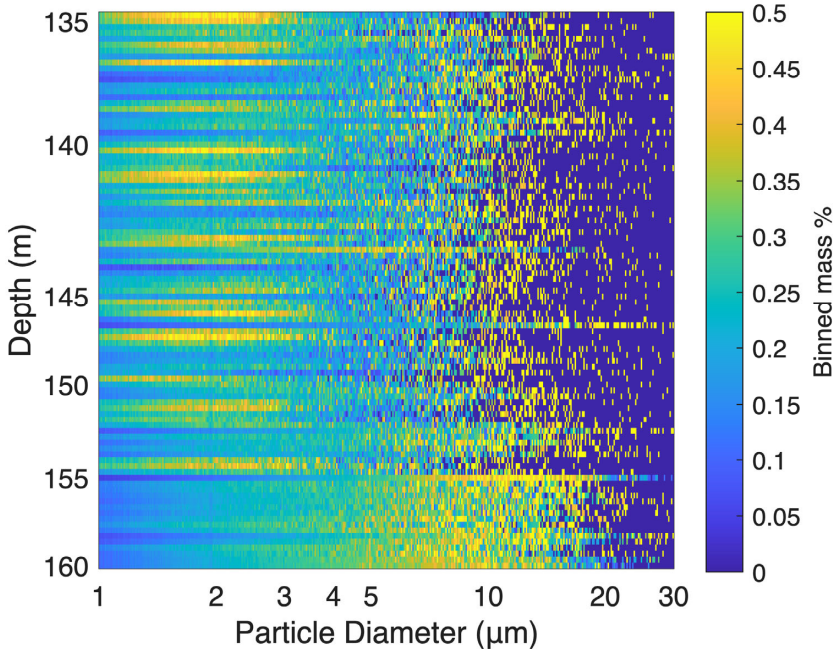

Figure 4. Particle size distribution variability with depth. Each row represents a discrete subsample of ice from ALHIC1901 which has been measured for mass concentration and size distribution. The particle mass for each diameter range is represented by a pixel, which has been normalized by bin interval (natural log of the bin width) and the cumulative mass (1–30 µm diameter) for each respective sample. The pixels are colored according to the color bar and sum to 100% when

https://doi.org/10.5194/egusphere-2026-2434
Preprint. Discussion started: 19 June 2026

integrated across a sample row. Note the depth axis is not to scale and is more representative of the sampling frequency.

In contrast, the bottom 5 m of the core contains a widespread increased proportion of coarse particles that dominate the concentration signal (Fig. 4). Notably, one sample (ALHIC1901 228_3) displays a sharp transition in the particle size at 154.9 m, coincident with the abrupt increase in total particle concentration described above (Fig. 3). At this transitional depth, the mass contribution increases significantly to 10–20 µm particle diameters. Samples below this depth are dominated by ~10 µm modal diameters. Stable water isotopes show no such shift (Fig. S1), suggesting that the sudden transition is a post-depositional process rather than a recorded climate signal. The convergence in elevated mass concentrations and coarse particle dominance in the deepest ice strongly suggests that insoluble particulate matter below ~155 m is influenced by proximity to bedrock, with a major contribution from entrained basal material rather than dust transported by aeolian processes.

Another possibility is that the bottom 5 m layer of ice is stratigraphically unrelated to the ice above it, representing a different flow path history. If this were the case, the ice in this basal layer may have formed during a distinct climate period or interacted with bedrock topography in a different location prior to intersecting with the overlying ice sheet layers. Higher dust concentrations are observed at shallower depths of 142.23 m and 147.02 m exceeding 800 and 600 ppb respectively (Fig. 3). This suggests that there may be folding and intersecting deep ice flow which disturbs the stratigraphic layers of the preserved ice, a behavior which has been noted previously with respect to chronology and depth (Shackleton et al., 2025). Future geochemical analysis (e.g., Sr-Nd isotope compositions) of the dust in this ice could shed more light into the source of the higher dust mass concentrations observed near the bed.

3.3 Interglacial bias: Where have all the glacial periods gone?

A central question arising from the insoluble particle record of ALHIC1901 is whether a primary climate signal is preserved within the particle mass concentration record, or if post-depositional processes and/or biases in formation and preservation have impacted the archive. Detailed physical characterization of ice core dust from the Allan Hills deposited during the MIS 6 to 5e climate transition (ALHIC1903; Carter et al., accepted) allows us to compare the dust

https://doi.org/10.5194/egusphere-2026-2434
Preprint. Discussion started: 19 June 2026

characteristics observed in older Allan Hills ice (ALHIC1901) to gauge whether the dust is within the expected range of concentrations and size distributions, or whether subglacial sediment input is occurring. Previous work at the Allan Hills on the ALHIC1903 ice core has shown that ice from the MIS 6 glacial period contained both greater amounts of fine particles (1–5 μm), in excess of 100 ppb, and that these particles typically made up more than 60% of the total particle mass concentration (Carter et al., accepted). The opposite being true for interglacial ice from MIS 5e, which contained fine particle concentrations <100 ppb that generally made up less than <60% of the total particle mass concentration. Applying these relative ranges of particle mass concentration during known climate regimes to our samples suggests that ice meeting glacial thresholds is quite rare with only 10 samples satisfying both conditions, most of which are centered around ~135–142 m with two samples at ~146 m (Fig. 5). The majority of samples (n = 44) are more consistent with interglacial characteristics. Notably, there are also an array of samples throughout the core and for nearly all depths below ~150 m which contain greater concentrations of fine particles (>100 ppb) but with fine particles contributing only 47% of the total mass on average. These dusty yet coarse samples are atypical for either expected glacial or interglacial regimes but could represent a mixture of ice from both climatic periods or an injection of basal material at greater depths, or a combination of both. The absence of expected glacial peaks in dust mass concentration could also be a byproduct of less intense glacial periods for the pre-MPT ice compared to the post-MPT time interval.

https://doi.org/10.5194/egusphere-2026-2434
Preprint. Discussion started: 19 June 2026

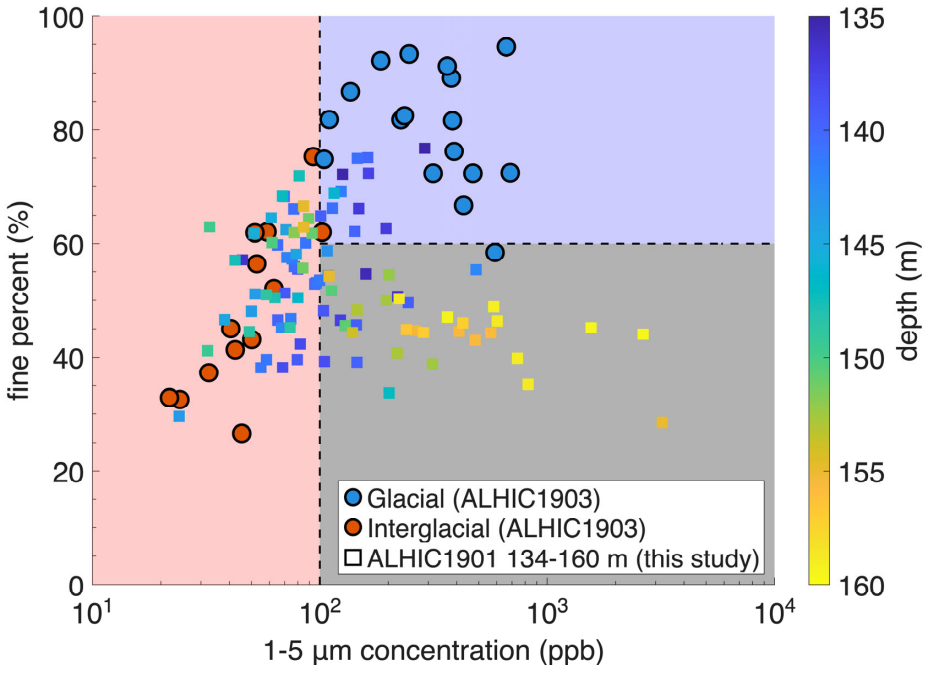

Figure 5. Percent of fine particles (1–5/1–20 µm) with respect to absolute concentrations of fine particles (1–5 µm) from ALHIC1901 (this study) and ALHIC1903 (Carter et al., accepted). Samples from ALHIC1903 are separated based on corresponding glacial (blue circles) and interglacial (red circles) climate period. Samples from ALHIC1901 are shown as smaller squares and are colored based on their depth within the core. Colored background indicates typical glacial (blue) and interglacial (red) bounds for percent of fine particles (>60%) and fine dust concentration (<100 ppb), respectively, for dust from ALHIC1903 (Carter et al., accepted). The gray background indicates a range in fine percent and dust concentration not typically observed during glacial-interglacial periods at the Allan Hills. The 1–20 µm denominator is used for consistency with the established MIS 6 and MIS 5e Allan Hills dust records, where particles >20 µm were excluded to isolate the aeolian signal (Carter et al., accepted).

A subset of these samples was dated using the $^{40}Ar_{atm}$ geochronometer at Princeton University (Bender et al., 2008, Yan et al., 2019; Shackleton et al., 2025) and provide additional context for evaluating these patterns. The relative gas age uncertainty of ~60 kyr (1σ) is based on the analytical precision of the geochronometer and is an order of magnitude larger than the expected difference in the age of the gas and ice (Shackleton et al., 2025). Therefore, the dating uncertainty effectively captures the ice age, and we use $^{40}Ar_{atm}$ ages as the best estimate for ice age in this study. Of the subset of samples with $^{40}Ar_{atm}$ ages, 33 samples fell within the age range

https://doi.org/10.5194/egusphere-2026-2434
Preprint. Discussion started: 19 June 2026

comparable with the high temporally resolved dust record from EDC (Lambert et al., 2008) (Fig. 6). While the Allan Hills ice core particle mass concentrations are broadly consistent with the magnitude and range of dust mass concentrations observed in the EDC record from 532 ka to about 800 ka, the expected peaks in concentration which should occur during glacial periods are largely missing. We use the term "long snapshots" to describe this interglacial bias, where a smoothing effect has either erased or muted the see-saw pattern of high glacial and low interglacial dust concentrations characteristic of established ice core records.

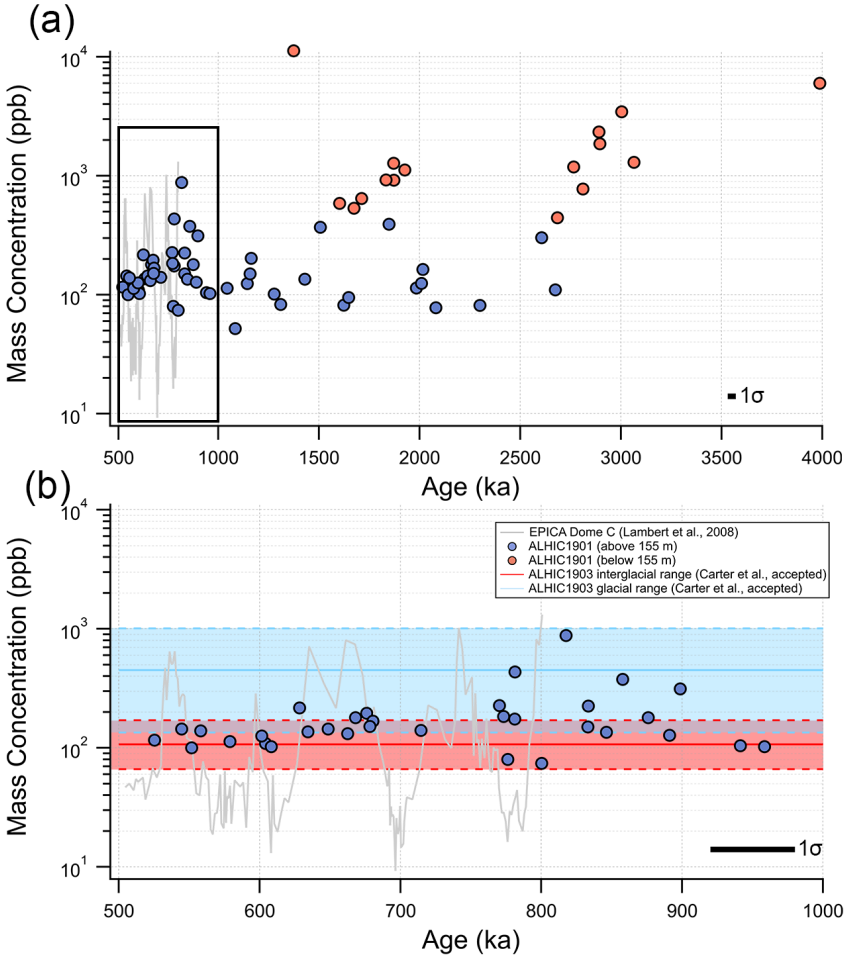

Figure 6. (**a-b**) Temporal variability of particle mass concentration (ppb) from ALHIC1901 samples that also contain $^{40}Ar_{atm}$ ages (Shackleton et al., 2025). Relative age uncertainties are ~60 kyr (1σ). The dust mass concentration record from interior East Antarctic ice core EDC (0.7–20 μm diameter) is shown as a gray line for comparison (Lambert et al., 2008). Samples presumed to

https://doi.org/10.5194/egusphere-2026-2434
Preprint. Discussion started: 19 June 2026

be unaffected by basal contamination (depths > 5 m from bed) are shown as blue circles, whereas those likely contaminated (depth < 5 m from bed) are represented by orange circles. (**b**) Zoomed inset of (**a**) for better comparison to the EDC record alongside average glacial (blue shaded rectangle with blue solid line representative of average and blue dashed lines representative of upper and lower bounds) and interglacial period (red shaded rectangle with red solid line representative of average and red dashed lines representative of upper and lower bounds) dust mass concentration ranges from nearby ALHIC1903 (1–20 μm; Carter et al., accepted). Note the different x-axis limits.

The lower frequency of glacial samples is also consistent with extreme accumulation and ablation patterns. The Allan Hills experiences prolonged intervals of very low accumulation and high ablation rates (Yan et al., 2021). Shackleton et al. (2025) noted that glacial $\delta^{18}O_{ice}$ values in the ALHIC1901 core were largely absent. This was attributed to a combination of lower accumulation rates during glacial intervals and an averaging across glacial–interglacial cycles due to the highly thinned layers. Similarly, glacial concentrations of greenhouse gases (CO_2 and CH_4) are overwhelmingly absent at depths below 142 m (Marks-Peterson et al., 2026), suggesting the averaging of gas compositions over glacial cycles. The absence of distinct glacial dust peaks in ALHIC1901 likely reflects similar processes to those described above (Fig. 6), with low ice accumulation rates during glacial periods accompanied by high ablation rates at the Allan Hills. This could either result in the erasure of high glacial period dust concentrations during or soon after deposition or could conversely result in a smoothing of glacial and interglacial dust concentrations due to extremely low accumulation rates and stratigraphic thinning. Both processes could be invoked as a cause for the observation of these “long snapshots” in our dust mass concentration record (Fig. 5), as the lack of ice accumulation during glacial periods typically characterized by high dust deposition may essentially fail to record this climatic history or result in the scouring of dust from the ice surface before firn transitions into ice. Similarly, dust scouring from the surface due to high ablation rates would essentially average dust mass concentrations. The complex ice flow regime at the Allan Hills results in a thinning of stratigraphic layers which would further average or combine the glacial and interglacial dust concentrations within relatively thin ice core subsections. Although given the small subsections (50–150 g) measured in this study, this latter mechanism is unlikely to be the dominant process impacting the dust record.

These observations indicate that while the ALHIC1901 dust record struggles to preserve discrete glacial maxima, it does widely retain a strong interglacial signal. This interglacial bias reflects the preferential preservation of ice formed under higher ice accumulation conditions, while

https://doi.org/10.5194/egusphere-2026-2434
Preprint. Discussion started: 19 June 2026

ice deposited during glacial periods is either underrepresented, mixed, or removed entirely. As a result, dust mass concentrations within ALHIC1901 above ~155 m are best interpreted as recording interglacial environmental conditions superimposed with varying degrees of glacial ice preservation, rather than a continuous archive of glacial–interglacial dust variability. This is supported by the lack of an expected correlation between dust concentration and $\delta^{18}O_{ice}$ (Shackleton et al., 2025) measured on the same ice core samples (Fig. S1).

3.4 Unusual carbonate mineralogy of basal ice

To investigate the mineralogical characteristics of the ice, a subset of particle samples were isolated and analyzed using Scanning Electron Microscopy (SEM) and Electron Dispersive Spectroscopy (EDS). The SEM and EDS analyses on these discrete samples highlighted the presence of quartz and silicate minerals, iron-bearing phases, and, notably, carbonate minerals within the basal ice of ALHIC1901 (Fig. 7, Fig. S4). The mere presence of carbonate minerals in the lower portion of ALHIC1901 is puzzling, as Southern Hemisphere mid-latitude sourced dust reaching Antarctica has been noted to have virtually no carbonate minerals present (Delmonte et al., 2004), as these minerals are most likely to be dissolved during transit prior to deposition on the ice sheet surface. However, recent work has demonstrated a minor presence of carbonate minerals in select samples of MIS 2 ice from Dome B (Delmonte et al., 2017) and late Holocene firn from Talos Dome (Sala et al., 2008). These minerals were attributed to exposed continental shelves during a glacial period lowstand and deflation from the surface of nearby sea ice, respectively. Carbonate minerals are typically expected to dissolve during the long-range aeolian transport process (de Angelis et al., 1992). This is in contrast to the Greenland Ice Sheet, which receives a higher proportion of continental derived dust with more source areas rich in carbonate minerals present throughout the Northern Hemisphere (Delmonte et al., 2004).

https://doi.org/10.5194/egusphere-2026-2434
Preprint. Discussion started: 19 June 2026

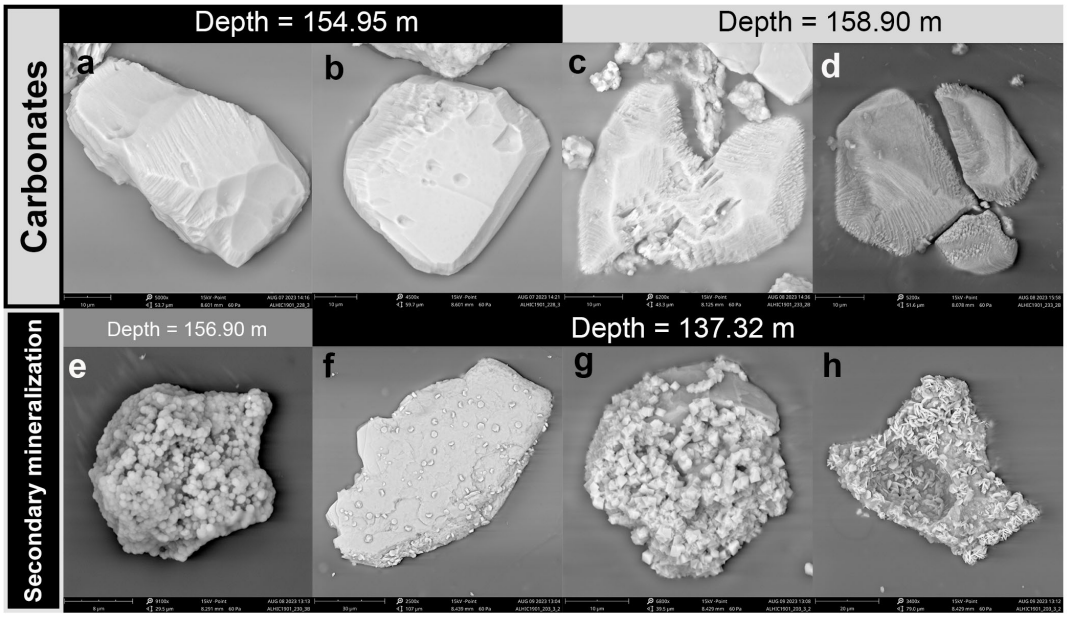

Figure 7. Scanning electron microscope images of particles from the following ALHIC1901 ice core samples: (**a**–**b**) ALHIC1901_228_3 (depth 154.95 m), identified via EDS as likely intact carbonates, (**c**–**d**) ALHIC1901_233_2B (depth 158.90 m) with signs of mineral dissolution indicating ongoing *in situ* chemical weathering of carbonates, and (**e**) ALHIC1901_230_3B (depth 156.90 m) and (**f**–**h**) ALHIC1901_203_3_2 (depth 137.32 m) particles with small grains forming on existing mineral surfaces highlighting secondary mineralization observed in the bottom 25 meters of ALHIC1901. Supporting EDS results are shown in Supplementary Fig. 4.

The observation of intact carbonate minerals at ~155 m and partially dissolved carbonate minerals at ~159 m in ALHIC1901 is therefore surprising (Fig. 7). While these carbonate minerals could represent enhanced cyclonic conditions over sea ice or greater exposure of continental shelves and/or glaciogenic sedimentary deposits, the predominant coarse particle sizes (>10 μm; Fig. 7) more likely suggest a non-transoceanic aeolian provenance. Potential explanations for the carbonate presence are the weathering and entrainment of carbonate-bearing sediment deposits. Glaciofluvial and or glaciolacustrine deposits scattered throughout the Transantarctic Mountains such as the Sirius Group, which consists of Neogene aged till and diamictites (Hambrey et al., 2003) generally ranging in calcium carbonate content from ~0.1 to 1.3 wt % (Passchier, 2004), could plausibly be one source of the carbonate minerals found in the ice core. Another alternative possibility is that Ca-bearing minerals such as plagioclase or pyroxene were exposed to chemical weathering in the subglacial environment and formed carbonate crusts *in situ*. Carbonate crusts on

https://doi.org/10.5194/egusphere-2026-2434
Preprint. Discussion started: 19 June 2026

rock or soil surfaces, while reportedly limited spatially, have been observed in Antarctica (Lacelle et al., 2024) and are primarily found throughout the McMurdo Dry Valleys (Claridge & Campbell, 1977; Campbell & Claridge, 2009; Campbell et al., 2013; Lyons et al., 2020). The carbonate crusts are thought to typically form via kinetic evaporation (Lacelle et al., 2024), implying the presence of liquid water at some point in time either as snowmelt or glacial meltwater. Carbonate crusts on rock or clast surfaces could then be subsequently mechanically weathered and entrained at some point in the ice sheet history before undergoing further chemical weathering processes *in situ* within the ice.

3.5 Possible englacial chemical alteration and dust reactivity

Mineralogical and textural characteristics of ice core dust can be used to infer the presence of *in situ* chemical weathering of dust particles occurring in an ice core post-deposition (e.g., Baccolo et al., 2021b). For example, the mineral jarosite has been observed in the Talos Dome ice core from East Antarctica and has been cited as evidence of ice metamorphism and re-crystallization at great depths (Baccolo et al., 2021a), and a process indicative of englacial dust relocation allowing for chemical reactions and mineral neo-formation to occur. SEM and EDS measurements on the Allan Hills ice allowed for a qualitative analysis of mineral grain morphology and mineralogy to probe whether the deep ice core dust had been affected by englacial chemical weathering associated with sediment entrainment and ice metamorphism due to the complex flow history at this site.

In all imaged samples, the particles are characterized by diverse grain morphologies ranging from low sphericity and angular (Fig. 7c, h), high sphericity and subangular (Fig. 7e, g), moderate sphericity and subangular (Fig. 7b, d), to low sphericity and very angular (Fig. 7a, f). Most of the observed particles are angular to subangular in shape with a low degree of roundness, which may imply either a short transport distance from the dust source to the ice sheet or the potential dissolution and precipitation of species *in situ* (Baccolo et al., 2021a).

SEM imagery reveals evidence of secondary mineralization in several samples spanning a range of sample depths. Sample ALHIC1901_203_3 at a depth of ~137 m contains Fe-S bearing minerals (Fig. S4f–h), including cubic pyrite precipitated on the outer portion of a pre-existing mineral grain (Figs. 6g, S4g) and a flat platy mineral which could potentially be jarosite adhering

https://doi.org/10.5194/egusphere-2026-2434
Preprint. Discussion started: 19 June 2026

to a pre-existing mineral grain (Figs. 7h, S4h). The larger particles (e.g., >20 μm) are more prevalent in samples ALHIC1901 228_3, 230_3B, 233_2B, which are located within 5 m of bedrock where elevated concentrations of 1–30 μm diameter particle mass concentration were also observed. Other examples of secondary mineralization include small spherical silica (Si)-rich minerals formed on the surface of a pre-existing mineral particle (Fig. 7e) possibly representing amorphous Si or opal which has been interpreted in other subglacial precipitates in East Antarctica as indicative of the presence of calcite-saturated subglacial meltwater (Piccione et al., 2022).

We measured bulk pH of meltwater samples without CO_2 equilibration using a GroLine Soil pH Tester throughout preparation for Coulter Counter analysis, pH values averaged around 5.58 ± 0.27 (n=43) across the depth range of 135-158 m, reflecting the slightly acidic conditions of snow from atmospheric transport and potentially the equilibration of bubbles and ambient air with meltwater during sample preparation (Fig. S2). This is consistent with measurements of pH from Greenland ice cores which range from 4.71 to 5.75 though such measurements account for CO_2 solubility and equilibration (Kjær et al., 2016, Pasteris et al., 2011). In the TALDICE ice core, the mineral jarosite was identified which should only form under acidic (pH<4) aqueous conditions but instead is inferred to have formed *in situ* within the TALDICE ice core through extreme diagenetic conditions within the ice (Baccolo et al, 2021). While highly acidic ice below pH of 4 was not directly observed in our bulk pH measurements for the Allan Hills ice, it is possible that micro acidic environments form within thin water films at the mineral-ice grain boundary, a process noted at triple junctions within ice grain boundaries (Fukazawa et al., 1998 and Mulvaney et al., 1988).

While intact carbonate minerals were observed at ~155 m depth (Fig. 7a–b), these minerals exhibit chemical zoning with selective dissolution along zoned rims in a deeper sample at ~159 m depth, closer to the bed (Fig. 7c–d). Together, the occurrence of chemical weathering may indicate that current environmental conditions close to and at bedrock act as a "geochemical reactor," wherein post-depositional transformations may alter particle size distributions due to particles migration to ice-grain boundaries and subsequently flocculating together (e.g., Iliescu and Baker, 2009), or ice that has been transported towards the ice surface from a deeper location (Baccolo et al., 2021b).

https://doi.org/10.5194/egusphere-2026-2434
Preprint. Discussion started: 19 June 2026

3.6 Processes affecting the CO_2 concentrations in basal layers and implications for paleoclimate reconstructions

Elevated CO_2 and CH_4 concentrations associated with high dust concentrations are observed in several previous ice cores drilled from Greenland (Muhl et al., 2023; Brook et al., 1996; Souchez et al., 1995, 1997; Smith et al., 1997). The adsorption of CH_4 onto dust particles has also been proposed as a mechanism for excess CH_4 production during the wet extraction process (Lee et al., 2019). Positive correlations between cell counts and measurements of dust concentrations has been interpreted as evidence of methanogenesis through *in situ* metabolism occurring in Greenland ice (Tung et al., 2005). The mineralogy of dust transported to Antarctica is primarily silicate minerals whereas Greenland dust contains a higher proportion of carbonate bearing dust sourced from Asia, resulting in a lower correlation between artifactually elevated greenhouse gas concentrations due to reactions with entrained dust in Antarctic ice cores (Anklin et al., 1995). However, the presence of carbonate minerals and potential evidence for *in situ* chemical alteration in ALHIC1901 suggest that similar processes may operate locally within deep ice at the Allan Hills BIA.

In ALHIC1901, non-atmospheric concentrations of CO_2 were previously identified based on anomalous $\delta^{13}C$-CO_2 (< -7.1‰, Marks-Peterson et al., 2026). Anomalous $\delta^{13}C$ measurements have also been observed in other ice cores nearby ALHIC1901, with the bottom 7 m of ALHIC1502 and ALHIC1503 showing evidence of respired CO_2 (Yan et al., 2019). Significant respiration was noted in ALHIC1901 in all depths below ~152 m and a few sporadic depths between ~125–142 m (Marks-Peterson et al., 2026). For samples where particle mass concentrations were also available, we observe a strong correlation between non-atmospheric CO_2 concentrations and particle mass concentration (Fig. 8). This link suggests that the observed elevated greenhouse gas concentrations could be due to processes such as microbial respiration or oxidation of organic carbon as has been observed at other sites (Tung et al., 2005; Anklin et al., 1995). Elevated CO_2 concentrations due to biological respiration have been observed in Antarctic glacial environments associated with high sediment content in basal ice due to proximity to bedrock (Montross et al., 2013). Additionally, subsequent chemical weathering of entrained carbonate grains due to micro acidic conditions within the ice would result in *in situ* production of excess CO_2 (Anklin et al., 1995) and could partially explain the relationship between particle concentration and CO_2 within the ALHIC1901 ice core (Fig. 8). While SEM analysis was limited

https://doi.org/10.5194/egusphere-2026-2434
Preprint. Discussion started: 19 June 2026

to a subset of samples, carbonate minerals may be more widespread than directly observed, particularly if basal ice is folded or intersects higher in the core.

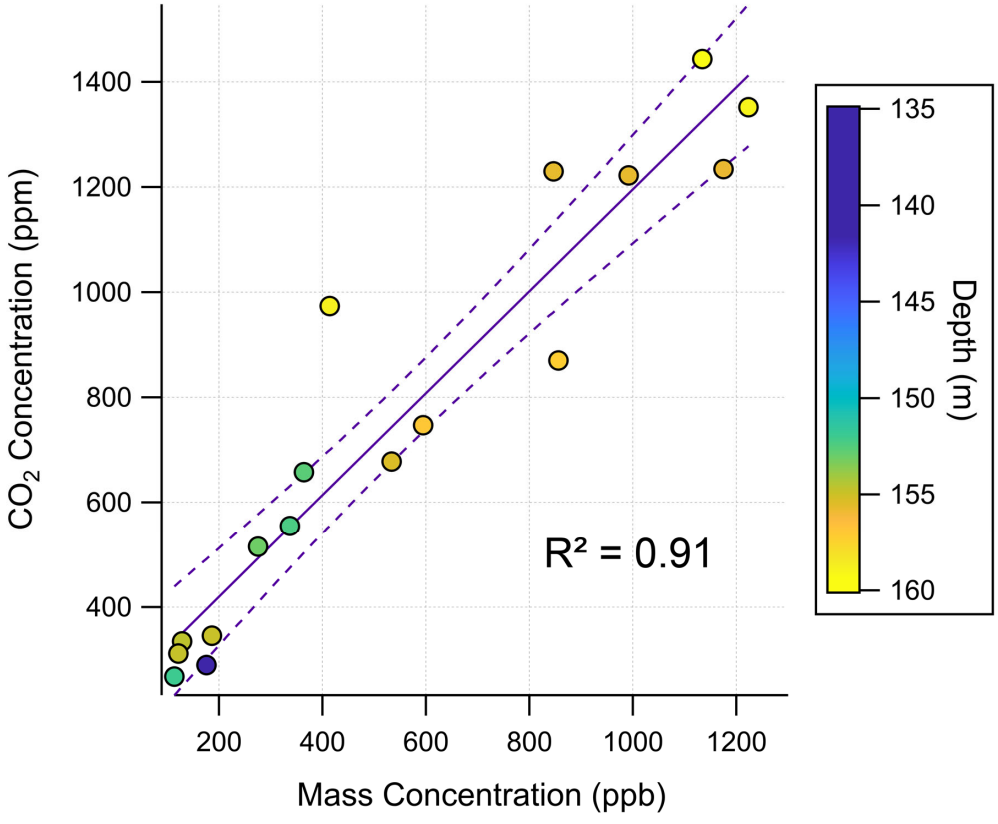

Figure 8. Particle mass concentrations (ppb) in the 1-15 µm diameter size fraction alongside altered CO_2 concentrations measured at Oregon State University (Marks-Peterson et al., 2026). These concentrations are presumed to be elevated from a non-atmospheric source based on anomalous $\delta^{13}C$-CO_2 (< -7.1‰). The 1–15 µm size fraction best captures this relationship; discrete size bin analysis shows that particles >15 µm do not contribute to the observed trend (Fig. S5). Two samples with anomalously high particle mass concentrations greater than 5000 ppb were excluded from the plot; these outliers do not conform to the observed linear relationship and likely represent additional complications due to their uniquely high particle mass concentrations. The solid purple line is the best linear fit for enriched CO_2 samples (R^2 = 0.91), and the purple dashed lines indicate the 95% confidence interval.

https://doi.org/10.5194/egusphere-2026-2434
Preprint. Discussion started: 19 June 2026

4 Conclusions

This study highlights that the climatic interpretations of dust preserved in the ice core record at the Allan Hills, Antarctica are complicated by two distinct processes tied to the unique glaciological and environmental conditions of this site. Elevated particle concentrations and size distributions in the bottom 5 m of ALHIC1901 are likely due to non-aeolian input through basal ice-rock interactions and subglacial particle entrainment. Above this depth, measurements appear overwhelmingly characteristic of interglacial periods through comparisons with established ice core records encompassing similar age ranges or local environmental conditions. This process is related to the low net accumulation and high ablation rates at the Allan Hills, which preferentially attenuate or erase glacial period ice, producing these "long snapshots" observed in the dust mass concentration record. Secondary mineralization and chemical alteration are also observed at various depths throughout the core using SEM imaging and EDS techniques, which highlights the complex chemical reactions taking place either at the basal ice-rock interface or *in situ*, as well as the link between particle concentration and greenhouse gas concentrations. Despite these complications, it may be possible to glean relevant climate signals through a multiproxy and filtering approach, which includes the application of particle size distribution and mineralogical assessment. Other promising methods to probe and possibly disentangle these complications is the application of novel approaches such as microstructural analysis (Faria et al., 2010) and three-dimensional electrical or conductivity measurements (Kirkpatrick et al., 2025), both of which can provide constraints on the structure, dip, and orientation of layering within the ice core.

Data Availability

Particle mass concentration and grain size distribution data will be available on United States Antarctic Program – Data Center (USAP-DC).

Author Contributions

AJC and SMA conceptualized this study. SMA and EJB acquired funding for this study. JAH and EJB funded the fieldwork and provided access to samples. AJC and SS cut the ice subsamples. AC and AJC conducted the Coulter Counter measurements, pH measurements, and SEM imaging. AJC processed data. AC, AJC, and JMP analyzed the data and created the figures shown in this manuscript. JAH, EJB, SS, LK, and JIC contributed to the interpretation of the results. AC, AJC, and SMA wrote and prepared the manuscript with contributions from all coauthors.

https://doi.org/10.5194/egusphere-2026-2434
Preprint. Discussion started: 19 June 2026

Acknowledgments

The fieldwork for sample collection was funded by NSF grants ANT-1744993 awarded to JAH and ANT-1745006 awarded to EJB. This work was supported by the Center for Oldest Ice Exploration, an NSF Science and Technology Center (NSF 2019719). We thank the NSF Office of Polar Programs, the NSF Office of Integrative Activities, and Oregon State University for financial and infrastructure support, and the NSF Antarctic Infrastructure and Logistics Program, the US Ice Drilling Program, the NSF Ice Core Facility, and the Antarctic Support Contractor for logistical support. We thank the U.S. Ice Drilling Program for support activities through NSF Cooperative Agreement 1836328. JIC acknowledges support from NSF grant OPP-2024132. Special thanks to E. Morton and T. Kuhl for their significant drilling contributions; J. Epifanio and J. Morgan for ice core processing in the field; and A. Zajicek for field camp management. We thank R. Nunn, C. LaBombard, T. Carr, and C. Kershaw for their assistance processing these complex samples at the NSF Ice Core Facility. We thank E. Chin for allowing access to the Phenom Pro XL SEM. We acknowledge the entire COLDEX team for their valuable support, guidance, and feedback. Thanks to S. Akiba for compiling Allan Hills water isotope data, and many thanks to the COLDEX Research Experience for Undergraduates and, in particular, K. Rahilly who provided research support and mentorship to A. Choi. Geospatial support for this work provided by the Polar Geospatial Center under NSF-OPP awards 1043681, 1559691, 2129685, and 2434541.

https://doi.org/10.5194/egusphere-2026-2434
Preprint. Discussion started: 19 June 2026

References

Aarons, S. M., Aciego, S. M., Gabrielli, P., Delmonte, B., Koornneef, J. M., Wegner, A., and Blakowski, M. A.: The impact of glacier retreat from the Ross Sea on local climate: Characterization of mineral dust in the Taylor Dome ice core, East Antarctica, Earth and Planetary Science Letters, 444, 34–44, https://doi.org/10.1016/j.epsl.2016.03.035, 2016.

Aarons, S. M., Aciego, S. M., Arendt, C. A., Blakowski, M. A., Steigmeyer, A., Gabrielli, P., Sierra-Hernández, M. R., Beaudon, E., Delmonte, B., Baccolo, G., May, N. W., and Pratt, K. A.: Dust composition changes from Taylor Glacier (East Antarctica) during the last glacial-interglacial transition: A multi-proxy approach, Quaternary Science Reviews, 162, 60–71, https://doi.org/10.1016/j.quascirev.2017.03.011, 2017.

Aarons, S. M., Aciego, S. M., McConnell, J. R., Delmonte, B., and Baccolo, G.: Dust Transport to the Taylor Glacier, Antarctica, During the Last Interglacial, Geophysical Research Letters, 46, 2261–2270, https://doi.org/10.1029/2018GL081887, 2019.

Albani, S., Delmonte, B., Maggi, V., Baroni, C., Petit, J.-R., Stenni, B., Mazzola, C., and Frezzotti, M.: Interpreting last glacial to Holocene dust changes at Talos Dome (East Antarctica): implications for atmospheric variations from regional to hemispheric scales, Climate of the Past, 8, 741–750, https://doi.org/10.5194/cp-8-741-2012, 2012.

Anklin, M., Barnola, J.-M., Schwander, J., Stauffer, B., and Raynaud, D.: Processes affecting the CO2 concentrations measured in Greenland ice, Tellus B, 47, 461–470, https://doi.org/10.1034/j.1600-0889.47.issue4.6.x, 1995.

Baccolo, G., Delmonte, B., Di Stefano, E., Cibin, G., Crotti, I., Frezzotti, M., Hampai, D., Iizuka, Y., Marcelli, A., and Maggi, V.: Deep ice as a geochemical reactor: insights from iron speciation and mineralogy of dust in the Talos Dome ice core (East Antarctica), The Cryosphere, 15, 4807–4822, https://doi.org/10.5194/tc-15-4807-2021, 2021a.

Baccolo, G., Delmonte, B., Niles, P. B., Cibin, G., Di Stefano, E., Hampai, D., Keller, L., Maggi, V., Marcelli, A., Michalski, J., Snead, C., and Frezzotti, M.: Jarosite formation in deep Antarctic ice provides a window into acidic, water-limited weathering on Mars, Nature Communications, 12, 436, https://doi.org/10.1038/s41467-020-20705-z, 2021b.

Basile, I., Grousset, F. E., Revel, M., Petit, J. R., Biscaye, P. E., and Barkov, N. I.: Patagonian origin of glacial dust deposited in East Antarctica (Vostok and Dome C) during glacial stages 2, 4 and 6, Earth and Planetary Science Letters, 146, 573–589, https://doi.org/10.1016/S0012-821X(96)00255-5, 1997.

Bender, M. L., Barnett, B., Dreyfus, G., Jouzel, J., and Porcelli, D.: The contemporary degassing rate of 40Ar from the solid Earth, Proceedings of the National Academy of Sciences, 105, 8232–8237, https://doi.org/10.1073/pnas.0711679105, 2008.

Betzer, P. R., Carder, K. L., Duce, R. A., Merrill, J. T., Tindale, N. W., Uematsu, M., Costello, D. K., Young, R. W., Feely, R. A., Breland, J. A., Bernstein, R. E., and Greco, A. M.: Long–range transport of giant mineral aerosol particles, Nature, 336, 568–571, https://doi.org/10.1038/336568a0, 1988.

Bintanja, R.: On the glaciological, meteorological, and climatological significance of Antarctic blue ice areas, Reviews of Geophysics, 37, 337–359, https://doi.org/10.1029/1999RG900007, 1999.

Blakowski, M. A., Aciego, S. M., Delmonte, B., Baroni, C., Salvatore, M. C., and Sims, K. W. W.: A Sr-Nd-Hf isotope characterization of dust source areas in Victoria Land and the McMurdo Sound sector of Antarctica, Quaternary Science Reviews, 141, 26–37, https://doi.org/10.1016/j.quascirev.2016.03.023, 2016.

https://doi.org/10.5194/egusphere-2026-2434
Preprint. Discussion started: 19 June 2026

Bressac, M., Guieu, C.: Post-depositional processes: What really happens to new atmospheric iron in the ocean's surface? Global Biogeochemical Cycles, 27(3), 859-870, 2013.

Brook, E. J., Sowers, T., and Orchardo, J.: Rapid Variations in Atmospheric Methane Concentration During the Past 110,000 Years, Science, 273, 1087–1091, https://doi.org/10.1126/science.273.5278.1087, 1996.

Campbell, I. B. and Claridge, G. G. C.: Antarctic Permafrost Soils, in: Permafrost Soils, edited by: Margesin, R., Springer Berlin Heidelberg, Berlin, Heidelberg, 17–31, https://doi.org/10.1007/978-3-540-69371-0_2, 2009.

Campbell, I., Claridge, G., Campbell, D., and Balks, M.: The Soil Environment of the Mcmurdo Dry Valleys, Antarctica, vol. 72, 297–322, https://doi.org/10.1029/AR072p0297, 2013.

Carter, A.J., Aarons, S.M., Schnaubelt, J.C., Tabor, C.R., Higgins, J.A., Shackleton, S.A., Epifanio, J.A., Morgan, J.D., Koornneef, J.M., Davies, G.R., Gabrielli, P., Choi, A., Severinghaus, J.P., Brook, E.J., Introne, D., Marks Peterson, J.C., Sutter, J. Evidence for diminished Ross Ice Shelf and West Antarctic Ice Sheet during the Last Interglacial at the Allan Hills, Antarctica, Nature Geoscience, accepted.

Claridge, G. G. C. and Campbell, I. B.: THE SALTS IN ANTARCTIC SOILS, THEIR DISTRIBUTION AND RELATIONSHIP TO SOIL PROCESSES, Soil Science, 123, 1977.

Clark, P. U. and Pollard, D.: Origin of the Middle Pleistocene Transition by ice sheet erosion of regolith, Paleoceanography, 13, 1–9, https://doi.org/10.1029/97PA02660, 1998.

Clark, P.U., Archer, D., Pollard, D., Blum, J.D., Rial, J.A., Brovkin, V., Mix, A.C., Pisias, N.G., Roy, M.: The middle Pleistocene transition: characteristics, mechanisms, and implications for long-term changes in atmospheric pCO2, Quaternary Science Reviews, 25(23-24), 2006.

Dadic, R., Schneebeli, M., Bertler, N. A. N., Schwikowski, M., and Matzl, M.: Extreme snow metamorphism in the Allan Hills, Antarctica, as an analogue for glacial conditions with implications for stable isotope composition, Journal of Glaciology, 61, 1171–1182, https://doi.org/10.3189/2015JoG15J027, 2015.

Delmonte, B., Basile-Doelsch, I., Petit, J.-R., Maggi, V., Revel-Rolland, M., Michard, A., Jagoutz, E., and Grousset, F.: Comparing the Epica and Vostok dust records during the last 220,000 years: stratigraphical correlation and provenance in glacial periods, Earth-Science Reviews, 66, 63–87, https://doi.org/10.1016/j.earscirev.2003.10.004, 2004a.

Delmonte, B., Petit, J. R., Andersen, K. K., Basile-Doelsch, I., Maggi, V., and Ya Lipenkov, V.: Dust size evidence for opposite regional atmospheric circulation changes over east Antarctica during the last climatic transition, Climate Dynamics, 23, 427–438, https://doi.org/10.1007/s00382-004-0450-9, 2004b.

Delmonte, B., Robert Petit, J., Basile-Doelsch, I., Jagoutz, E., and Maggi, V.: 6. Late quaternary interglacials in East Antarctica from ice-core dust records, in: Developments in Quaternary Sciences, vol. 7, edited by: Sirocko, F., Claussen, M., Sánchez Goñi, M. F., and Litt, T., Elsevier, 53–73, https://doi.org/10.1016/S1571-0866(07)80031-5, 2007.

Delmonte, B., Andersson, P. S., Hansson, M., Schöberg, H., Petit, J. R., Basile-Doelsch, I., and Maggi, V.: Aeolian dust in East Antarctica (EPICA-Dome C and Vostok): Provenance during glacial ages over the last 800 kyr, Geophysical Research Letters, 35, https://doi.org/10.1029/2008GL033382, 2008.

Delmonte, B., Baroni, C., Andersson, P. S., Schoberg, H., Hansson, M., Aciego, S., Petit, J.-R., Albani, S., Mazzola, C., Maggi, V., and Frezzotti, M.: Aeolian dust in the Talos Dome ice

https://doi.org/10.5194/egusphere-2026-2434
Preprint. Discussion started: 19 June 2026

core (East Antarctica, Pacific/Ross Sea sector): Victoria Land versus remote sources over the last two climate cycles, Journal of Quaternary Science, 25, 1327–1337, https://doi.org/10.1002/jqs.1418, 2010.

Delmonte, B., Baroni, C., Andersson, P. S., Narcisi, B., Salvatore, M. C., Petit, J. R., Scarchilli, C., Frezzotti, M., Albani, S., and Maggi, V.: Modern and Holocene aeolian dust variability from Talos Dome (Northern Victoria Land) to the interior of the Antarctic ice sheet, Quaternary Science Reviews, 64, 76–89, https://doi.org/10.1016/j.quascirev.2012.11.033, 2013.

Elderfield. H., Ferretti, P., Greaves, M., Crowhurst, S., McCave, I.N., Hodell, D., Piotrowski, A.M.: Evolution of Ocean Temperature and Ice Volume Through the Mid-Pleistocene Climate Transition, Science, 337(6095), 704-709, 2012.

Faria, S. H., Freitag, J., and Kipfstuhl, S.: Polar ice structure and the integrity of ice-core paleoclimate records, Quaternary Science Reviews, 29, 338–351, https://doi.org/10.1016/j.quascirev.2009.10.016, 2010.

Fukazawa, H., Sugiyama, K., Mae, S., Narita, H., and Hondoh, T.: Acid ions at triple junction of Antarctic ice observed by Raman scattering, Geophysical Research Letters, 25, 2845–2848, https://doi.org/10.1029/98GL02178, 1998.

Gabriel, I., Plunkett, G., Abbott, P. M., Behrens, M., Burke, A., Chellman, N., Cook, E., Fleitmann, D., Hörhold, M., Hutchison, W., McConnell, J. R., Óladóttir, B. A., Preiser-Kapeller, J., Sliwinski, J. T., Sugden, P., Twarloh, B., and Sigl, M.: Decadal-to-centennial increases of volcanic aerosols from Iceland challenge the concept of a Medieval Quiet Period, Communications Earth & Environment, 5, 194, https://doi.org/10.1038/s43247-024-01350-6, 2024.

Goodge, J. W., Severinghaus, J. P., Johnson, J., Tosi, D., and Bay, R.: Deep ice drilling, bedrock coring and dust logging with the Rapid Access Ice Drill (RAID) at Minna Bluff, Antarctica, Annals of Glaciology, 62, 324–339, https://doi.org/10.1017/aog.2021.13, 2021.

Hambrey, M. J., Webb, P.-N., Harwood, D. M., and Krissek, L. A.: Neogene glacial record from the Sirius Group of the Shackleton Glacier region, central Transantarctic Mountains, Antarctica, GSA Bulletin, 115, 994–1015, https://doi.org/10.1130/B25183.1, 2003.

Harvey, R. P., Dunbar, N. W., McIntosh, W. C., Esser, R. P., Nishiizumi, K., Taylor, S., and Caffee, M. W.: Meteoritic event recorded in Antarctic ice, Geology, 26, 607–610, https://doi.org/10.1130/0091-7613(1998)026<0607:MERIAI>2.3.CO;2, 1998.

Higgins, J. A., Kurbatov, A. V., Spaulding, N. E., Brook, E., Introne, D. S., Chimiak, L. M., Yan, Y., Mayewski, P. A., and Bender, M. L.: Atmospheric composition 1 million years ago from blue ice in the Allan Hills, Antarctica, Proceedings of the National Academy of Sciences, 112, 6887–6891, https://doi.org/10.1073/pnas.1420232112, 2015.

Iliescu, D. and Baker, I.: Effects of impurities and their redistribution during recrystallization of ice crystals, Journal of Glaciology, 54, 362–370, https://doi.org/10.3189/002214308784886216, 2008.

Jaccard, S. L., Hayes, C. T., Martínez-García, A., Hodell, D. A., Anderson, R. F., Sigman, D. M., and Haug, G. H.: Two Modes of Change in Southern Ocean Productivity Over the Past Million Years, Science, 339, 1419–1423, https://doi.org/10.1126/science.1227545, 2013.

Kjær, H. A., Vallelonga, P., Svensson, A., Elleskov L. Kristensen, M., Tibuleac, C., Winstrup, M., and Kipfstuhl, S.: An Optical Dye Method for Continuous Determination of Acidity in Ice Cores, Environ. Sci. Technol., 50, 10485–10493, https://doi.org/10.1021/acs.est.6b00026, 2016.

https://doi.org/10.5194/egusphere-2026-2434
Preprint. Discussion started: 19 June 2026

Kaplan, M. R., Licht, K. J., Lamp, J. L., Winckler, G., Schaefer, J. M., Graly, J. A., Kassab, C. M., and Schwartz, R.: Paleoglaciology of the central East Antarctic Ice Sheet as revealed by blue-ice sediment, Quaternary Science Reviews, 302, 107718, https://doi.org/10.1016/j.quascirev.2022.107718, 2023.

Kassab, C. M., Licht, K. J., Petersson, R., Lindbäck, K., Graly, J. A., and Kaplan, M. R.: Formation and evolution of an extensive blue ice moraine in central Transantarctic Mountains, Antarctica, Journal of Glaciology, 66, 49–60, https://doi.org/10.1017/jog.2019.83, 2020.

Kirkpatrick, L., Carter, A., Marks-Peterson, J., Shackleton, S., and Fudge, T. J.: Three-Dimensional Multitrack Electrical Conductivity Method for Interpretation of Complex Ice Core Stratigraphy, Journal of Glaciology, 1–25, https://doi.org/10.1017/jog.2025.10081, 2025.

Knight, P. G.: The basal ice layer of glaciers and ice sheets, Quaternary Science Reviews, 16, 975–993, https://doi.org/10.1016/S0277-3791(97)00033-4, 1997.

Kuhl, T. W., Johnson, J. A., Shturmakov, A. J., Goetz, J. J., Gibson, C. J., and Lebar, D. A.: A new large-diameter ice-core drill: the Blue Ice Drill, Annals of Glaciology, 55, 1–6, https://doi.org/10.3189/2014AoG68A009, 2014.

Lacelle, D., Christy, M., Faucher, B., Sobron, P., and Andersen, D.: Palaeo-environmental significance of evaporative calcite crusts in the Untersee Oasis, East Antarctica, Antarctic Science, 36, 149–159, https://doi.org/10.1017/S0954102024000075, 2024.

Lambert, F., Delmonte, B., Petit, J. R., Bigler, M., Kaufmann, P. R., Hutterli, M. A., Stocker, T. F., Ruth, U., Steffensen, J. P., and Maggi, V.: Dust-climate couplings over the past 800,000 years from the EPICA Dome C ice core, Nature, 452, 616–619, https://doi.org/10.1038/nature06763, 2008.

Lee, J. E., Edwards, J. S., Schmitt, J., Fischer, H., Bock, M., and Brook, E. J.: Excess methane in Greenland ice cores associated with high dust concentrations, Geochimica et Cosmochimica Acta, 270, 409–430, https://doi.org/10.1016/j.gca.2019.11.020, 2020.

Lyons, B., Foley, K., Carey, A., Diaz, M., Bowen, G., and Cerling, T.: The isotopic geochemistry of CaCO3 encrustations in Taylor Valley, Antarctica: Implications for their origin, Acta geographica Slovenica, 60, 125–139, https://doi.org/10.3986/AGS.7233, 2020.

Mahowald, N., Kohfeld, K., Hansson, M., Balkanski, Y., Harrison, S. P., Prentice, I. C., Schulz, M., and Rodhe, H.: Dust sources and deposition during the last glacial maximum and current climate: A comparison of model results with paleodata from ice cores and marine sediments, Journal of Geophysical Research: Atmospheres, 104, 15895–15916, https://doi.org/10.1029/1999JD900084, 1999.

Marks-Peterson, J., Shackleton, S., Higgins, J., Severinghaus, J., Yan, Y., Buizert, C., Kalk, M., Beaudette, R., Hishamunda, V., Eves, D., Carter, A., Kurbatov, A., Epifanio, J., Morgan, J., Nesbitt, I., Bender, M., and Brook, E.: Broadly stable atmospheric CO2 and CH4 levels over the past 3 million years, Nature, 651, 647–652, https://doi.org/10.1038/s41586-025-10032-y, 2026.

Martin, J. H.: Glacial-interglacial CO2 change: The Iron Hypothesis, Paleoceanography, 5, 1–13, https://doi.org/10.1029/PA005i001p00001, 1990.

Martínez-Garcia, A., Rosell-Melé, A., Geibert, W., Gersonde, R., Masqué, P., Gaspari, V., and Barbante, C.: Links between iron supply, marine productivity, sea surface temperature, and CO2 over the last 1.1 Ma, Paleoceanography, 24, https://doi.org/10.1029/2008PA001657, 2009.

https://doi.org/10.5194/egusphere-2026-2434
Preprint. Discussion started: 19 June 2026

Martínez-Garcia, A., Rosell-Melé, A., Jaccard, S. L., Geibert, W., Sigman, D. M., and Haug, G. H.: Southern Ocean dust–climate coupling over the past four million years, Nature, 476, 312–315, https://doi.org/10.1038/nature10310, 2011.

Martínez-García, A., Sigman, D. M., Ren, H., Anderson, R. F., Straub, M., Hodell, D. A., Jaccard, S. L., Eglinton, T. I., and Haug, G. H.: Iron Fertilization of the Subantarctic Ocean During the Last Ice Age, Science, 343, 1347–1350, https://doi.org/10.1126/science.1246848, 2014.

Masson-Delmotte, V., Buiron, D., Ekaykin, A. A., Frezzotti, M., Gallée, H., Jouzel, J., Krinner, G., Landais, A., Motoyama, H., Oerter, H., Pol, K., Pollard, D., Ritz, C., Schlosser, E., Sime, L. C., Sodemann, H., Stenni, B., Uemura, R., and Vimeux, F.: Water stable oxygen isotope records from six Antarctic ice core sites for the present and last interglacial periods, PANGAEA, https://doi.org/10.1594/PANGAEA.785228, 2011.

McGee, D., Broecker, W. S., and Winckler, G.: Gustiness: The driver of glacial dustiness?, Quaternary Science Reviews, 29, 2340–2350, https://doi.org/10.1016/j.quascirev.2010.06.009, 2010.

Medina-Elizalde, M. & Lea, D. W. The mid-Pleistocene transition in the tropical. Science 310, 1009–1012, 2005.

Montross, S. N., Skidmore, M., Tranter, M., Kivimäki, A.-L., and Parkes, R. J.: A microbial driver of chemical weathering in glaciated systems, Geology, 41, 215–218, https://doi.org/10.1130/G33572.1, 2013.

Mühl, M., Schmitt, J., Seth, B., Lee, J. E., Edwards, J. S., Brook, E. J., Blunier, T., and Fischer, H.: Methane, ethane, and propane production in Greenland ice core samples and a first isotopic characterization of excess methane, Climate of the Past, 19, 999–1025, https://doi.org/10.5194/cp-19-999-2023, 2023.

Ng, J., Severinghaus, J., Bay, R., and Tosi, D.: Evaluating marine dust records as templates for optical dating of Oldest Ice, Climate of the Past, 20, 1437–1449, https://doi.org/10.5194/cp-20-1437-2024, 2024.

Past Interglacials Working Group of PAGES. Interglacials of the last 800,000 years. Reviews of Geophys*ics.* 54, 162–219, 2016.

Passchier, S.: Variability in Geochemical Provenance and Weathering History of Sirius Group Strata, Transantarctic Mountains: Implications for Antarctic Glacial History, Journal of Sedimentary Research, 74, 607–619, https://doi.org/10.1306/022704740607, 2004.

Pasteris, D. R., McConnell, J. R., and Edwards, R.: High-Resolution, Continuous Method for Measurement of Acidity in Ice Cores, Environ. Sci. Technol., 46, 1659–1666, https://doi.org/10.1021/es202668n, 2012.

Piccione G, Blackburn T, Tulaczyk S, Rasbury ET, Hain MP, Ibarra DE, Methner K, Tinglof C, Cheney B, Northrup P, Licht K. Subglacial precipitates record Antarctic ice sheet response to late Pleistocene millennial climate cycles. Nature Communications, 15;13(1):5428. doi: https://doi.org/10.1038/s41467-022-33009-1, 2022.

Shackleton, S., Hishamunda, V., Davidge, L., Brook, E., Peterson, J. M., Carter, A., Aarons, S., Kurbatov, A., Introne, D., Yan, Y., Nesbitt, I. M., Buizert, C., Steig, E. J., Schauer, A. J., Morgan, J., Neff, P. D., Epifanio, J. A., Severinghaus, J., Bender, M., and Higgins, J. A.: Miocene and Pliocene ice and air from the Allan Hills blue ice area, East Antarctica, Proceedings of the National Academy of Sciences, 122, e2502681122, https://doi.org/10.1073/pnas.2502681122, 2025.

https://doi.org/10.5194/egusphere-2026-2434
Preprint. Discussion started: 19 June 2026

Shackleton, N. J. & Opdyke, N. D. Oxygen isotope and palaeomagnetic evidence for early Northern Hemisphere glaciation. Nature 270, 216–219, 1977.

Sigman, D. M., Hain, M. P., and Haug, G. H.: The polar ocean and glacial cycles in atmospheric CO2 concentration, Nature, 466, 47–55, https://doi.org/10.1038/nature09149, 2010.

Smith, H. J., Wahlen, M., Mastroianni, D., Taylor, K., and Mayewski, P.: The CO2 concentration of air trapped in Greenland Ice Sheet Project 2 ice formed during periods of rapid climate change, Journal of Geophysical Research: Oceans, 102, 26577–26582, https://doi.org/10.1029/97JC00163, 1997.

Souchez, R., Lemmens, M., and Chappellaz, J.: Flow-induced mixing in the GRIP basal ice deduced from the CO2 and CH4 records, Geophysical Research Letters, 22, 41–44, https://doi.org/10.1029/94GL02863, 1995.

Souchez, R.: The buildup of the ice sheet in central Greenland, Journal of Geophysical Research: Oceans, 102, 26317–26323, https://doi.org/10.1029/96JC01558, 1997.

Spaulding, N. E., Spikes, V. B., Hamilton, G. S., Mayewski, P. A., Dunbar, N. W., Harvey, R. P., Schutt, J., and Kurbatov, A. V.: Ice motion and mass balance at the Allan Hills blue-ice area, Antarctica, with implications for paleoclimate reconstructions, Journal of Glaciology, 58, 399–406, https://doi.org/10.3189/2012JoG11J176, 2012.

Spaulding, N. E., Higgins, J. A., Kurbatov, A. V., Bender, M. L., Arcone, S. A., Campbell, S., Dunbar, N. W., Chimiak, L. M., Introne, D. S., and Mayewski, P. A.: Climate archives from 90 to 250ka in horizontal and vertical ice cores from the Allan Hills Blue Ice Area, Antarctica, Quaternary Research, 80, 562–574, https://doi.org/10.1016/j.yqres.2013.07.004, 2013.

Steffensen, J. P.: The size distribution of microparticles from selected segments of the Greenland Ice Core Project ice core representing different climatic periods, Journal of Geophysical Research: Oceans, 102, 26755–26763, https://doi.org/10.1029/97JC01490, 1997.

Tung, H. C., Bramall, N. E., and Price, P. B.: Microbial origin of excess methane in glacial ice and implications for life on Mars, Proceedings of the National Academy of Sciences, 102, 18292–18296, https://doi.org/10.1073/pnas.0507601102, 2005.

Yan, Y., Bender, M. L., Brook, E. J., Clifford, H. M., Kemeny, P. C., Kurbatov, A. V., Mackay, S., Mayewski, P. A., Ng, J., Severinghaus, J. P., and Higgins, J. A.: Two-million-year-old snapshots of atmospheric gases from Antarctic ice, Nature, 574, 663–666, https://doi.org/10.1038/s41586-019-1692-3, 2019.

Yan, Y., Brook, E. J., Kurbatov, A. V., Severinghaus, J. P., and Higgins, J. A.: Ice core evidence for atmospheric oxygen decline since the Mid-Pleistocene transition, Science Advances, 7, eabj9341, https://doi.org/10.1126/sciadv.abj9341, n.d.